Storing ions for collision studies

A static trap capable of storing ions for many hours—electrons for over a month—bids fair to bring the convenience of the chemist's reagent shelf to the study of ions and their interactions. The trap to store heavy ions developed at the Joint Institute of Laboratory Astrophysics, shown on the cover and in figure 1, is preferable for our work to its older cousin, the radiofrequency trap, in that it does not feed energy into the system it contains. Its usefulness is further enhanced by a nondestructive detection technique. Thus ends the era when our knowledge of ions and their interactions depended exclusively on analysis of plasmas, laboratory and natural, or the cleaner method of colliding beams.

We feel that these new methods are particularly appropriate for the study of the recombination of positive ions with electrons. Recombination, an old problem, plays a strong role in the ionization balance of stellar atmospheres, the development of laboratory plasmas and the evolution of ionic and molecular species in planetary atmospheres and interstellar matter. The importance of precise recombination measurements emerges from a few case histories:

▸ A serious discrepancy existed for many years in the electron temperature of the solar corona deduced by various methods. Doppler profiles of ion lines indicated kinetic temperatures of about two million degrees. The balance between the ionization and recombination rates (assuming only radiative recombination) gave temperatures three to four times lower. It was not until 1964 that Alan Burgess,[1] acting on a suggestion by Albrecht Unsöld, showed that inclusion of dielectronic recombination in the ionization-balance calculations, discussed below, brought the two determinations into harmony.

▸ Volume recombination between electrons and positive ions is often assumed[2] to be the dominant loss mechanism in high-pressure laser discharges. When an external source, such as an electron or uv photon beam, is used to maintain ionization, and the recombination coefficient is lowered, the laser's energy requirement is reduced. The cross section for recombination of H_3O^+ with electrons has recently been shown[3] to decrease much more rapidly with electron energy than had been thought typical (or even possible) for ions. Arthur Phelps[4] has used this to suggest that the presence of H_3O^+, or other ions that may behave similarly, could explain some observations[5] of low loss in some plasmas being investigated for laser purposes.

▸ The great number and complexity of molecules observed in interstellar space has led to a variety of proposed models to explain their formation. For a time gas-phase processes were considered too slow, and mechanisms involving formation on grains were considered more applicable. However, recent models, using measured and "typical" rates for gas-phase reactions, have led to reasonably consistent densities of the observed species. According to a model by Eric Herbst and William Klemperer[6] for dense interstellar clouds, a number of observed neutral molecules result from dissociative recombination (which we shall describe shortly) of electrons and positive ions; these include CH, NH, OH, H_2O, NH_3 and H_2CO. In this model, cosmic rays ionize the ambient neutral particles; the ions in turn undergo various reactions, primarily with the dominant species H and H_2, and electron-ion dissociative recombination is often the final step, yielding stable neutral molecules.

▸ The green line in the night sky and in aurorae was attributed as early as 1931 by Joseph Kaplan[7] to dissociative recombination of electrons and O_2^+ ions to give $O(^1S)$, the green line source. Similarly, the prominent feature in the airglows of Venus and Mars, the Cameron bands of CO, appears to result directly from dissociative recombination of electrons and CO_2^+. During eclipses, solar flares, and aurorae, when the sun rises and sets, and when there are man-made disturbances in the degree of ionization of the earth's atmosphere, ion densities move with some time constant to new levels. These levels of course strongly influence radio communications, which depend on reflection of radio waves from the ionized layers of the earth's atmosphere; the time for this change is mainly determined by recombination.

Recombination mechanisms

Numerous physical mechanisms lead to recombination; the three two-body processes that normally play a role are illustrated in figure 2. The first of these is *radiative recombination*, in which the electron simply radiates its excess energy, ending up in an excited state of the atom. Since the electron passes the ion in about 10^{-15} sec, while radiative times are of the order of 10^{-8} sec, the process has a low probability. Cross sections for it are about 10^{-20} cm^2; they decrease with electron energy E roughly as $1/E$. The process has not been measured directly, although radiative recombination data can sometimes be inferred from measurements of the reverse process, photoionization.

The second mechanism shown is *dielectronic recombination*. In this process an electron with just the right energy excites an electron of the ion core, and is itself left in a high Rydberg state of the resultant neutral atom. Such multiply excited states lie in the ionization continuum, as shown by the upper black lines in the figure;

Fred L. Walls is a staff member of the National Bureau of Standards time and frequency division and Gordon H. Dunn is an NBS staff member, Joint Institute for Laboratory Astrophysics Fellow and Professor Adjoint of the University of Colorado physics and astrophysics department.

Overcoming the limitations of plasma and colliding-beam techniques, the new static trap helps untangle the mechanisms by which positive ions recombine with electrons.

Fred L. Walls and Gordon H. Dunn

autoionization can occur, reversing the capture process. However, if the core excited state has a short radiative lifetime, and if the Rydberg state of the captured electron is high enough that interaction with the core electron is small, stabilization by radiation occurs before autoionization takes place. The result is an excited "neutral." This process can have a cross section 10^{-14} to 10^{-15} cm^2. However, because of the resonant nature of this process, the energy range for sizable cross sections is as narrow as a few meV. Dielectronic recombination has been invoked to help account for aspects of the ionization balance of high-temperature plasmas but has not been measured.

Only molecular ions are subject to neutralization by the third process, *dissociative recombination.* For diatomic molecules the internuclear separation R becomes an additional dimension. Again we see excited neutral states lying in the continuum but now, as the energy varies with R, they may be below the continuum at large R. In this case the excess energy brought in by the electron is carried away as kinetic energy of the dissociating partners. This takes place in 10^{-15} to 10^{-13} sec, compared to the autoionization time of about 10^{-14} sec, so the process can be very efficient; cross sections approach 10^{-13} cm^2 at low energies. Furthermore, the resonance peak is broad in this case, owing to the range of separations of the original molecular ions. Dissociative recombination is usually the dominant mechanism when molecular gases are present.

When densities become high enough for three-body collisions to be frequent, three-body recombination and third-body enhancement of the above mechanisms takes place. Dissociative recombination may be thought of as a process in which a potential third body is carried around with the ion.

Of the three two-body processes, dissociative recombination[8] is the only one that has been measured directly.

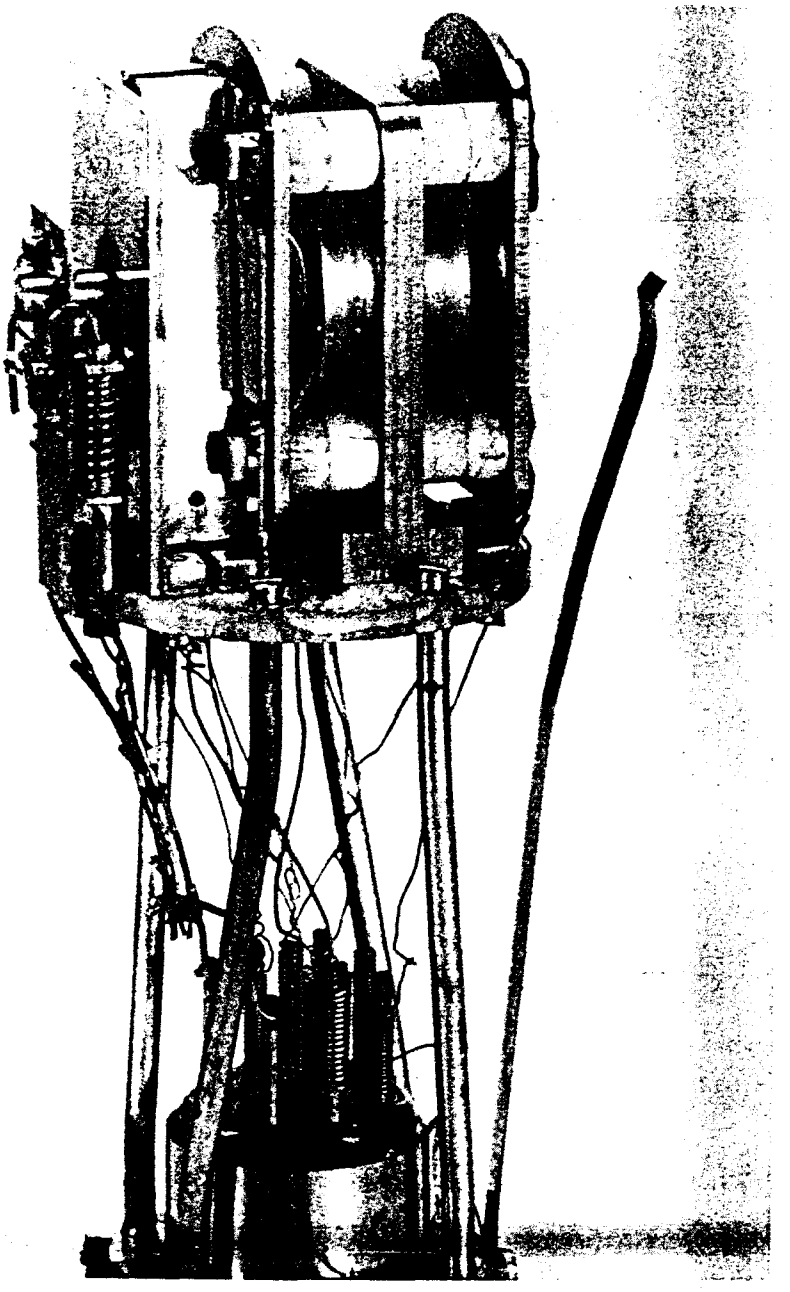

Ion trap in which ions have been stored for up to 28 hours. The hyperboloidal molybdenum electrodes consist of two end caps, whose surfaces are partly visible in the photo, and a ring. The structures seen on the left of the electrode assembly are the two electron guns, one a high-resolution trochoidal source and the other on-axis. Figure 1

Until very recently the only measurements on this process were the determinations of rate coefficients in plasmas (the rate coefficient is equal to the product of cross section and velocity averaged over a Maxwellian velocity distribution.) The most extensive and successful of these experiments have been those of Manfred A. Biondi and his coworkers, whose studies in this field have extended over a 25-year period.

Plasmas and colliding beams

In the techniques evolved by the Biondi group, a plasma is generated in a microwave cavity. When the excitation is turned off, one observes the time decays of the densities of electrons (determined from the conductivity) and of mass-selected ion species. A provision for microwave heating of the electrons allows the process to be studied as a function of electron temperature up to a few thousand degrees. The cavity itself can be heated, permitting recombination studies over an ambient temperature range to 450 K. The recombination rates are then computed from the electron- and ion-density decay rates.

Other methods used to obtain rate coefficients include heating a plasma with a traveling shock wave. Pairs of electrostatic probes placed along the shock tube permit the electron density to be observed as a function of distance and hence, time. With this technique, measurements can be made to temperatures of several thousand degrees.

Although the plasma measurements have been successful, the method has some shortcomings: (1) the energy range is limited; (2) the energy resolution is poor, obscuring details and precluding rate calculations for non-Maxwellian distributions; (3) the species one can study are limited; and (4) the internal states are not controllable.

Colliding-beam measurements can overcome the first three of these disadvantages to some degree; with regard to the last, however, the limitations of beams are even more severe than those of plasmas. In these experiments a beam of electrons is made to collide with a beam of ions. One observes the appearance of neutrals, the disappearance of ions or the appearance of photons from excited dissociation fragments. The experiments are difficult, and the only measurements using this technique appear to be those[9-11] on single-charged deuterium and nitrogen molecular ions, D_2^+ and N_2^+.

Two types of traps

With the trapped-ion technique, the focus of this article, we are able to study the same ions for times ranging to several hours. The limitations of the traditional techniques are overcome, but new limitations appear.

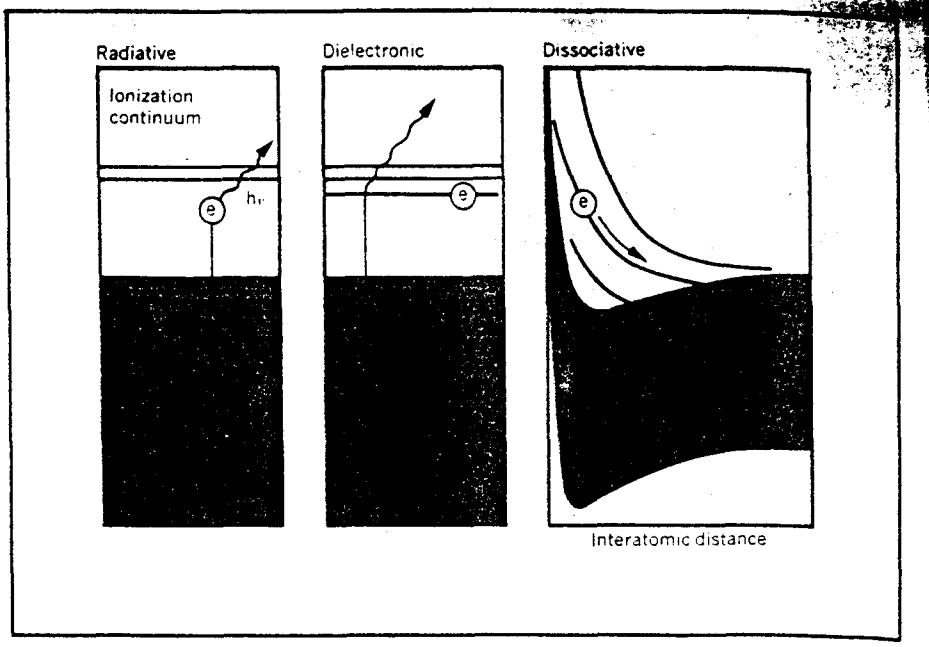

Two-body recombination processes differ in the way excess kinetic energy is accounted for. In radiative recombination (left), an electron combines with an ion, emitting a photon. In dielectronic recombination (center), the captured electron's energy excites a core electron, which radiates as it drops back to ground state. Kinetic energy is carried away by the fragments in dissociative recombination. Figure 2

Ion traps depend primarily on an electric saddle potential, illustrated in figure 3. This potential is achieved by machining the electrodes in the shape of hyperboloids of revolution, two end caps and a ring, illustrated in figure 4. Its axis of symmetry will be taken as the z-axis of a cylindrical coordinate system. Ions will oscillate in the parabolic well if their position and velocity vectors are along the z-axis; otherwise, they will drift out radially.

In the *radiofrequency trap* the potential is made to change sign before the ion can escape along r, then again before it can escape along z and so on. If the amplitude and frequency of the potential are chosen properly, the ion will be trapped. This method of containing ions by alternating electric-field gradients grew out of the work of Wolfgang Paul and his collaborators[12,13] on electric mass filters. Hans G. Dehmelt[14] reviewed the mechanics of such traps and their application in the rf spectroscopy of ions. Being active traps, they have the disadvantage of keeping the ions hot; furthermore, the alternating fields make them unsuitable for studying collisions of the trapped ions with monoenergetic electrons.

In our lab at JILA, we found the *static trap* to be a better tool for collision studies. To a dc potential of the same configuration as before we add a strong magnetic field. Our trap is thus a passive device, without the undesirable heating effect.

The magnetic field is in the z-direction. Now, when an axially oscillating ion starts to escape along r, it is turned back in a cyclotron orbit. The ions see crossed electric and magnetic fields and therefore they will precess, in $\mathbf{E} \times \mathbf{B}$ drift about the z-axis. The ions thus execute harmonic motion in the parabolic well along z, cyclotron motion in the equatorial plane and precession about the z-axis. In the absence of collisions they will be trapped indefinitely.

Tracing the history of the development of the static ion trap is difficult, as there are many references to unpublished work. The basic configuration is that used by Frans M. Penning[15] in the study of discharges. Solutions to the equations of motion were published by J. Byrne and Peter S. Farago,[16] who cite unpublished work of Otto R. Frisch (1954), Felix Bloch (1953) and Robert H. Dicke (1965). Dehmelt[14] has reviewed the technique and noted his own unpublished work (1961). The demonstration of the long trapping times that are achievable with this trap, however, awaited the work of Dehmelt and Walls,[17] who reported trapping times for electrons of about 3×10^6 sec, or five weeks! Of comparable importance was their demonstration of a nondestructive bolometric technique usable with the trap.

While the dc trap is not suitable for some kinds of ion spectroscopy because of the Zeeman splittings associated with its large magnetic fields, it appears to be ideally suited for collision studies. This is because, first, the passive nature of the trap allows the

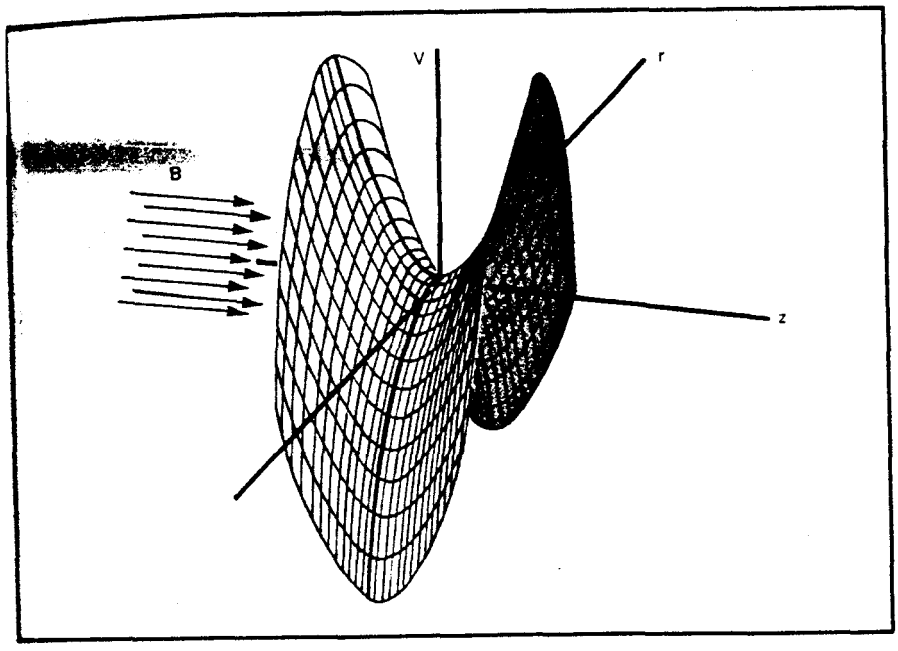

Distribution of potential in an ion trap as a function of the axial coordinate z and the radial distance r. The surface, a hyperbolic paraboloid, is defined by equation 1. A positive ion starting from rest on the z-axis would oscillate along it, but any radial displacement would lead to instability. This can be prevented by alternating the potential in an rf trap or adding a magnetic field B directed along the z-axis in the dc trap described in the text. Figure 3

ions to be cooled enough for energy resolutions as low as tens of meV; second, the long lifetimes create the possibility of preparing the ions in the desired state, and third, it allows us to make repeated nondestructive measurements of the numbers of the ion species present. Let us examine the trapping scheme and its realization in more detail.

Figure 4 shows a cross-sectional view of a dc ion trap with a block diagram of the associated detection system. The trap electrodes form equipotential surfaces given by

$$V = V_0(r^2 - 2z^2)/(a^2 + 2b^2) \qquad (1)$$

where $2a$ is the equatorial diameter of the ring, $2b$ is the axial distance between the end caps and V_0 is the potential applied to the ring electrode with respect to the end-cap electrodes. The dimensions of our trap are $2a$ = 1.25 cm and $2b$ = 0.76 cm.

Ions can be introduced into traps by a variety of means, including photoionization, colliding ion beams and collisions of an ion beam with the residual gas; the most common way is by electron impact on a selected gas within the trap.

The axial motion of the ions in the trap consists of harmonic oscillation at the frequency

$$\nu_z = [(qV_0/\pi^2 m)/(a^2 + 2b^2)]^{1/2} \qquad (2)$$

where q/m is the charge-to-mass ratio of the ions. As noted above, the ions also move in small circles at a frequency near the cyclotron frequency ν_c = [illegible]. In the third motion, the centers of the circles precess about the z-axis at angular frequency ν_m, which is related to the others through

$$2\nu_m^2 - 2\nu_c\nu_m + \nu_z^2 = 0$$

Because of the parabolic potentials and the assumed uniformity of the magnetic field, the motions are harmonic and the frequencies are independent of energy and position. For O_2^-, with potential $V_0 = -1$ V and $B = 1.15$ Tesla (1 T = 10^4 gauss), these are ν_c = 552 kHz, ν_z = 67 kHz and ν_m = 4.1 kHz.

Storage times and ion temperatures

The conditions for long-term ion storage are that the cyclotron radius be much smaller than a, that the radial magnetic force Bqv_r be larger than the radial electric force qE_r and that the magnetic and electric fields be cylindrically symmetrical, with coinciding axes. When these conditions are satisfied, the loss of ions is due solely to collisions with the background gas. The losses due only to diffusion induced by elastic scattering can be studied by measuring lifetimes of ions that do not react with the background gas. We have already noted the figure (3×10^6 sec) of Dehmelt and Walls for trapping times of electrons. Measurements on NH_4^+ with $B = 1.15$ T, V_0 = 1.8 V, and a background pressure of about 1×10^{-10} torr, presumably mostly hydrogen, yield lifetimes of about 10^5 sec (28 hours). Both indicate that diffusion effects can be made small in attainable vacuum. Typically, however, lifetimes are determined by such reactions with the background gas as charge transfer, clustering and ion-atom interchange, which lead to the more common lifetimes of about 10^3 sec (17 minutes).

These trapping times are long enough that most excited ions will have relaxed to the ground state. Notable exceptions are homonuclear molecular ions with vibrational modes that have lifetimes of about 10^7 sec (4 months). The ion-storage times are long enough to suggest future experiments in which the ions are pumped to excited states by means of a suitable form of radiation.

Coulomb collisions between trapped ions establish a Maxwellian distribution of kinetic energies in a time τ_c varying as $T_i^{3/2}m^{1/2}/nZ^4$ approximately.[18] For ion temperature T_i = 300 K, ion mass m = 30 amu, ion density n = 10^6 ions/cm^3, and valence $Z = q/e$ = 1, τ_c is about 0.02 sec. Because the trapping times are so much longer than τ_c, one can speak of an ion gas at a definite temperature T_i, and use the nondestructive detection technique described below.

The oscillatory axial motion of the ions causes an alternating image current to flow from one end cap to the other. If a resistor, R, is inserted in this current path, the Joule heating losses will cause the ions to approach the noise temperature of the resistor with a time constant, assuming no other external coupling to the ion motion, of about $8mb^2/q^2R$. The collective motion of N_i ions is damped N_i times as fast. Note that this process can be used either to heat or to cool the ions. Evaporation, that is, escape of fast ions from the trap, will also cool the ions efficiently to a mean energy of about one-tenth of the well depth, but there are not enough ions high in the tail of the distribution to have much effect beyond this. One might think of using collisions with the background gas as a cooling mechanism; however, these collisions would also cause an unwanted loss of ions by radial diffusion.

Nondestructive ion detection

The ions may be detected without loss by measuring the noise power in the image currents to one end cap of the trap. The very broad-band heterodyne detection circuit shown in figure 4 allows nondestructive detection of charged particles ranging from electrons to ions of several hundred amu. Individual ion species are manifest as peaks in the noise-power spectrum at the ions' axial oscillation frequency, given by equation 2.

The area under the peak is proportional to ion number multiplied by temperature, N_iT_i. Under conditions in which N_i is kept constant, one can investigate processes that raise the kinetic temperature of the ions. For ex-

ample, introducing power at the cyclotron frequency raises the ion temperature, which appears as an increase in the area of the noise-power peak. Similar heating of internal degrees of freedom that couple to the ionic center-of-mass motion can also be so detected.[17,19] Resonant cyclotron heating is used to measure ion q/m ratios with a resolution of about two parts in 10^4; it has been used, for example, to distinguish between H_2O^+ (m = 18.020 amu) and NH_4^+ (m = 18.044 amu).

On the other hand, when T_i is constant, one can study processes in which N_i changes. The wideband, nondestructive nature of the detection technique makes it possible to measure N_i repeatedly for each ion species of interest, and so keep track of both primary and competing processes. At this point we can see why this technique is so suitable for the study of ion recombination: The goal here is to find the decrease in ion number brought about by the introduction of electrons, while ion temperature remains constant.

The space charge limits the number of ions that can be stored in a trap; for the cited dimensions and a well depth of 1 V the maximum is about 3×10^6 ions. In recombination studies the need for a well defined interaction energy between electrons and stored ions reduces the useful radial extent of the trap; correspondingly, the maximum number of stored ions is reduced to about 10^5, at a density of about 10^7 ions per cubic centimeter.

Performing the experiment

Implementation of the storage technique described for the study of electron recombination with ions is relatively straightforward, once the trap and detector are operating properly. Electrons from either of two attached guns pass through a hole in the center of one end cap into the cavity, then through a collinear hole in the opposite end cap, finally to be absorbed by an electron collector at the far end. One electron gun, consisting simply of a cathode and series of apertures along the z-axis, provides an electron beam having an energy spread with full width at half maximum of about 120 meV. The other gun, similar to the trochoidal gun described by Aleksandar Stamatović and George S. Schultz,[20] uses $\mathbf{E} \times \mathbf{B}$ drift to disperse the electron velocities. With this gun, we have achieved an FWHM resolution of about 35 meV.

Ions are formed by electron bombardment of gas introduced into the system at pressures typically about 3×10^{-10} torr; the gas is then pumped out to 1×10^{-10} torr. Some of the ions studied are the product of the reaction of a primary ion with the background gas. For example, H_3O^+, an ion important in the ionosphere, interstellar space and some gas lasers, is formed from H_2O^+ by reacting with H_2O and other gases. After the ions are formed, we allow them to cool by coupling to an external resistor, as described above. The well depth, V_0, is then cut in half, and the ions cool further by evaporation to a mean energy, in the axial motion, of about 15 meV.

After cooling, the natural decay period τ_n, due to interactions with the background gas, is established by observing the area under the noise power peak as a function of time. We then introduce electrons of selected energy for a measured time t, long enough to give a measurable ion loss, after which the natural decay is again observed. Figure 5 shows this measurement sequence for a recombination measurement on NO^+ at an electron energy of 45 meV. This process is repeated at specific electron energies, and the cross section σ at each energy is calculated from the expression

$$\sigma = (eA/i_e t)[\ln(N_1/N_2) - t/\tau_n] \quad (3)$$

where i_e is the electron current, N_1 and N_2 are respectively the numbers of ions before and after introducing the electrons and A is a geometric quantity depending on the overlap of the electron beam with the ion cloud.

All the quantities in equation 3 except A are readily measured. In a simple model, A is just the area of the ion cloud seen by the electron beam. This quantity can be estimated, although not closer than a factor of two or three. A more precise procedure is to determine A by measuring the other quantities for a process of known cross section. The process chosen for this calibration is the recombination of electrons with O_2^+. However, instead of σ, only the recombination rate coefficient

$$\alpha = \int_0^\infty \sigma(v) v F(v) dv$$

is known. This quantity has been measured, with consistent results, by a number of investigators.[21] Since σ is known to within a factor A from the ion-trap measurements and equation 3, α/A can be calculated. Comparison to the known value of α yields A. We have recently developed a method for the direct measurement of A, and have built the apparatus for it.

An example of results of a recombination cross-section measurement[21] is shown in figure 6 for NO^+. Rate coefficients calculated from these experiments are in good agreement with afterglow measurements, but we have obtained them to much higher temperatures. The slope changes in the cross-section versus electron-energy plot indicate the importance of several repulsive levels of excited NO—the final states of the recombination process. We have made similar measurements for O_2^+, H_3O^+, NH_4^+, N_2H^+, and HCO^+.

Limitations and prospects

Recombination studies with the trapped-ion technique are revealing de-

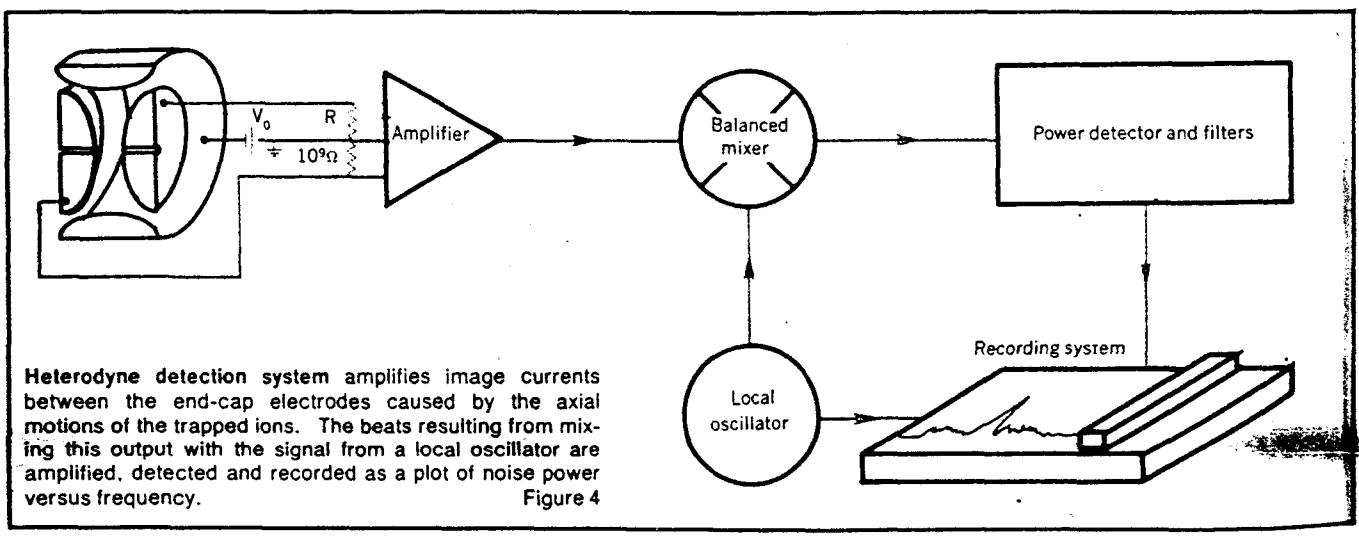

Heterodyne detection system amplifies image currents between the end-cap electrodes caused by the axial motions of the trapped ions. The beats resulting from mixing this output with the signal from a local oscillator are amplified, detected and recorded as a plot of noise power versus frequency. Figure 4

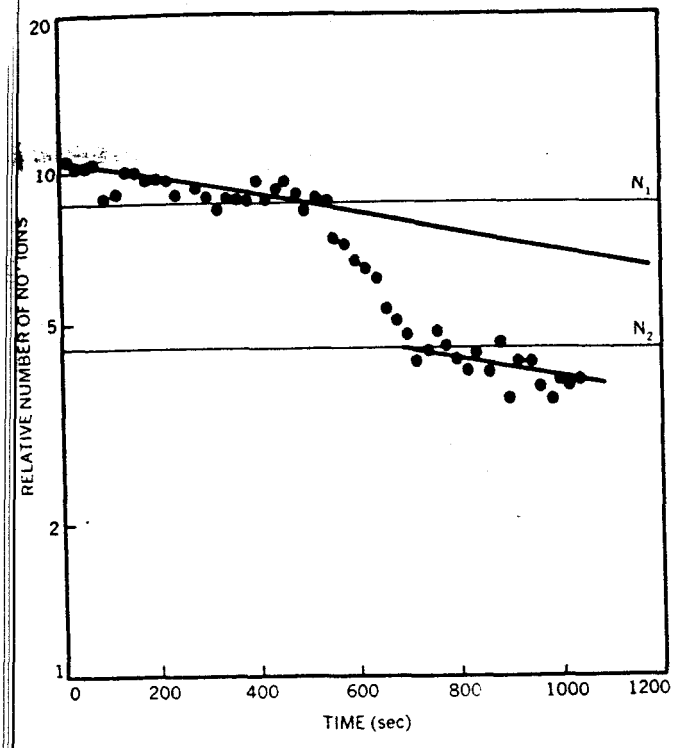

NO^+ ions recombine with 45-meV electrons to produce neutral molecules during time t indicated by vertical colored band. Decay before and after electron injection is due in part to collisions with background gas; this period, τ_n, is 2400 sec. Figure 5

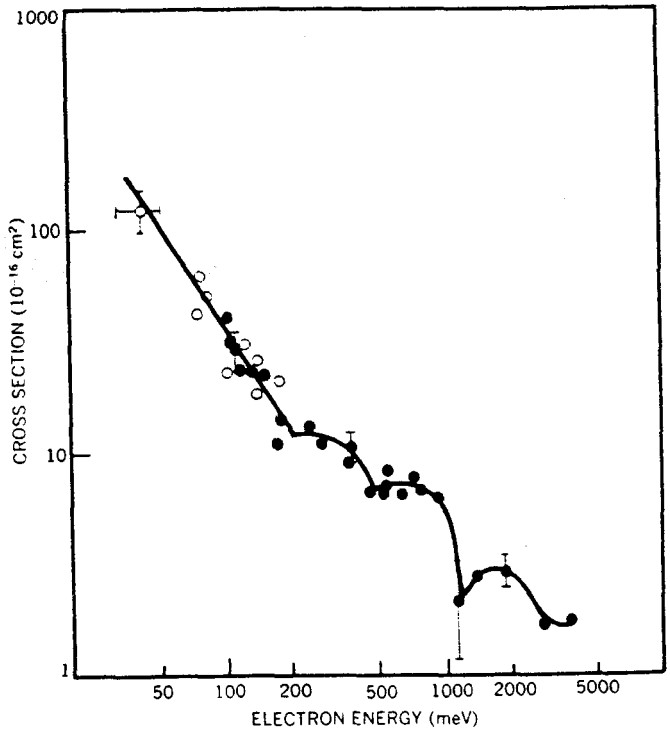

Recombination cross sections versus electron energy for the reaction $NO^+ + e \rightarrow$ neutrals. The high-resolution trochoidal electron gun was used for measurements indicated by solid circles; open circles represent the on-axis gun. Figure 6

tails that will help guide efforts to explain recombination cross sections theoretically. The technique provides a heretofore unavailable means of obtaining rate coefficients in practical plasmas, where the energy distribution of electrons is often other than Maxwellian. Ion storage extends the accessible energy range; it also provides an environment in which one can define more accurately the distribution of the internal states of the reacting ions.

The two main limitations of the technique applied to recombination are the limited storage times imposed by reactions of ions with background gas molecules, and the uncertainties attendant upon the indirect measurement of A.

We have mentioned the work of Dehmelt and coworkers on electrons[17,19,22] and described our work on ion recombination.[21] At least two other groups have also used dc ion techniques successfully. Michael D. McGuire and E. Norvel Fortson[23,24] have studied elastic, inelastic and spin-dependent collisions of stored electrons with selected atoms and molecules. Michael H. Prior[25] and Prior and Howard A. Shugart[26] have trapped ions for times of the order of 10 msec to measure the metastable He^- (2S) and Li^+ (2^1S) lifetimes.

What about spectroscopic investigations? We have seen that, while some are possible with dc ion traps, others are better suited for study with rf traps. On the other hand, studies on recombination and lifetimes, photoionization, photodissociation, ion-molecule reactions, electron-impact ionization and dissociation, and negative ions all appear to lend themselves to attack with static ion traps. Contemplating how appropriate these devices, coupled with nondestructive bolometric detection, are to this warehouseful of problems, we anticipate a future of increasing use for this new tool.

* * *

This work was initiated while Fred L. Walls was a University of Colorado research associate at JILA and supported by an NSF grant.

References

1. A. Burgess, Astrophys. J. 139, 776 (1964).
2. C. A. Fenstermacher, M. J. Nutter, W. T. Leland, K. Boyer, Appl. Phys. Lett. 20, 56 (1972).
3. R. A. Heppner, F. L. Walls, W. T. Armstrong, G. H. Dunn (submitted to Phys. Rev. A).
4. A. V. Phelps, Bull. Am. Phys. Soc. 18, 1518 (1973).
5. L. J. Denes, J. J. Lowke, Appl. Phys. Lett. 23, 130 (1973).
6. E. Herbst, W. Klemperer, Astrophys. J. 185, 505 (1973).
7. J. Kaplan, Phys. Rev. 38, 1048 (1931).
8. J. N. Bardsley, M. A. Biondi in *Advances in Atomic and Molecular Physics*, Vol. 6, (D. R. Bates and I. Esterman, eds.), Academic, New York, 1970, page 1.
9. B. Peart, K. T. Dolder, J. Phys. B. 6, L359 (1973).
10. M. K. Vogler, G. H. Dunn, Bull. Am. Phys. Soc. 15, 417 (1970).
11. G. Hagen, Air Force Cambridge Research Laboratory Report AFCRL-68-0649 (1968).
12. W. Paul, H. Steinwedel, Z. Naturforsch. 8a, 448 (1953).
13. W. Paul, M. Raether, Z. Physik 140, 262 (1955).
14. H. G. Dehmelt in *Advances in Atomic and Molecular Physics*, (D. R. Bates and I. Esterman, eds.), Academic, New York, vol. 3, 1967, page 53 and vol. 5, 1969, page 109.
15. F. M. Penning, Physica 3, 873 (1936).
16. J. Byrne, P. S. Farago, Proc. Phys. Soc. (London) 86, 801 (1965).
17. H. G. Dehmelt, F. L. Walls, Phys. Rev. Lett. 21, 127 (1968).
18. L. Spitzer, *Physics of Fully Ionized Gases*, Interscience, New York, 1956, page 76.
19. F. L. Walls, T. S. Stein, Phys. Rev. Lett. 31, 975 (1973).
20. A. Stamatović, G. J. Schulz, Rev. Sci. Instr. 41, 423 (1970).
21. F. L. Walls, G. H. Dunn, J. Geophys. Res. 79, 1911 (1974).
22. D. Wineland, P. E. Ekstrom, H. G. Dehmelt, Phys. Rev. Lett. 31, 1279 (1973).
23. M. D. McGuire, E. N. Fortson, Bull. Am. Phys. Soc. 18, 710 (1973).
24. E. N. Fortson, Bull. Am. Phys. Soc. 19, 15 (1974).
25. M. H. Prior, Phys. Rev. Lett. 29, 611 (1972).
26. M. H. Prior, H. A. Shugart, Phys. Rev. Lett. 27, 902 (1971). □